Published in final edited form as:
Nature. 2010 May 20; 465(7296): 316–321. doi:10.1038/nature08977.

Cell signalling by microRNA165/6 directs gene dose-dependent root cell fate

Annelie Carlsbecker[1,2,*], **Ji-Young Lee**[3,4,*], **Christina J. Roberts**[2], **Jan Dettmer**[1], **Satu Lehesranta**[1], **Jing Zhou**[3,4], **Ove Lindgren**[1,5], **Miguel A. Moreno-Risueno**[6], **Anne Vatén**[1], **Siripong Thitamadee**[1], **Ana Campilho**[1], **Jose Sebastian**[3], **John L. Bowman**[7], **Ykä Helariutta**[1,*], and **Philip N. Benfey**[6,*]

[1] Institute of Biotechnology/Department of Biosciences, University of Helsinki, FIN-00014, Finland [2] Department of Physiological Botany, Evolutionary Biology Center, Uppsala University, Norbyvägen 18D, SE-752 36 Uppsala, Sweden [3] Boyce Thompson Institute for Plant Research, Tower Road, Ithaca, New York 14853, USA [4] Graduate Field of Plant Biology, Cornell University, Ithaca, New York 14853, USA [5] Institute of Technology, University of Tartu, Tartu 50411, Estonia [6] Biology Department and IGSP Center for Systems Biology, Duke University, Durham, North Carolina 27708, USA [7] School of Biological Sciences, Monash University, Melbourne, Victoria 3800, Australia

Abstract

A key question in developmental biology is how cells exchange positional information for proper patterning during organ development. In plant roots the radial tissue organization is highly conserved with a central vascular cylinder in which two water conducting cell types, protoxylem and metaxylem, are patterned centripetally. We show that this patterning occurs through crosstalk between the vascular cylinder and the surrounding endodermis mediated by cell-to-cell movement of a transcription factor in one direction and microRNAs in the other. SHORT ROOT, produced in the vascular cylinder, moves into the endodermis to activate SCARECROW. Together these transcription factors activate *MIR165a* and *MIR166b*. Endodermally produced microRNA165/6 then acts to degrade its target mRNAs encoding class III homeodomain-leucine zipper transcription factors in the endodermis and stele periphery. The resulting differential distribution

Correspondence and requests for materials should be addressed to Y.H. (yrjo.helariutta@helsinki.fi) or P.N.B. (philip.benfey@duke.edu).
*These authors contributed equally to this work.

Supplementary Information is linked to the online version of the paper at www.nature.com/nature.

Author Contributions A.C. and J.-Y.L. contributed equally to this work, C.J.R., J.D., S.L. and J.Z. contributed equally to this work, O.L., M.A.M.-R. and A.V. contributed equally to this work, Y.H. and P.N.B. contributed equally to this work, and the name order was determined by raffle. A.C. designed and performed experiments to characterize HD-ZIP III transcription factors and miR165/6 in vascular patterning, J.-Y.L. identified and characterized the regulatory network of *SHR*, *SCR* and miR165/6 in the xylem patterning, C.J.R. analysed the miRNA expression by *in situ* hybridization and participated in *HD-ZIP III* mutant characterization. J.D. participated in the analysis of expression of *PHB* (including mutant forms) and other *HD-ZIP III* and generated *pCRE1::MIR165a* as well as participated in the generation of *J0571* lines to rescue *scr* and *shr*. S.L. participated in the *PHB* and *HD-ZIP III* expression analysis, *phb-7d* mutant characterization and generated the *pSCR::MIR165a* to rescue *scr*. J.Z. developed and characterized the xylem patterning led by non-mobile SHR and *PHB-m*. O.L. participated in the characterization of various *HD-ZIP III* mutant lines. M.A.M.-R. showed the non-cell autonomous action of non-mobile SHR. A.V. participated in positional cloning of *phb-7d* and establishment of the *J0571* lines to rescue *shr*. S.T. identified the *phb-7d* mutant. A.C. identified the *scr-6* allele. J.S. characterized *shr/scr* and *HD-ZIP III* double mutants and embryo expression patterns in GFP lines. J.L.B. shared informative non-published materials. Y.H. and P.N.B. participated in experimental design. A.C., J.-Y.L., Y.H. and P.N.B. wrote the manuscript. A.C. and J.-Y.L. are co-corresponding authors. All authors discussed the results and commented on the manuscript.

The authors declare no competing financial interests.

of target mRNA in the vascular cylinder determines xylem cell types in a dosage-dependent manner.

Organ development involves extensive communication between cells to orchestrate tissue specification and differentiation. This communication is often mediated by mobile molecules such as hormones, mRNAs, proteins and small RNAs1. In plants and animals, transcription factors and/or mRNAs have been shown to move to neighbouring cells and transfer positional information2¯6. Recently, small RNAs including microRNAs (miRNAs), small interfering RNAs (siRNAs) and *trans*-acting siRNAs (tasiRNAs) have emerged as potential mediators of cell-to-cell communication. Studies on the mobility of small RNAs have established that siRNAs and tasiRNAs are mobile, but evidence for the mobility of miRNAs has remained elusive2¯7.

The plant root is well suited to study cell-to-cell communication in tissue patterning. Along the radial axis, epidermis, cortex and endo-dermis form around the stele, in which the pericycle surrounds the vascular cylinder8 (Fig. 1a). Here, xylem develops in the centre and forms symmetric arcs towards the pericycle. Phloem develops between these arcs, with procambium/cambium, the vascular stem cells separating xylem and phloem. Xylem precursors in the centre differentiate into metaxylem with pitted secondary cell walls, while peripheral precursors differentiate as protoxylem with spiral walls. The strong evolutionary conservation of xylem patterning9,10 suggests the presence of common molecular mechanisms that constrain its organization.

Here we report a novel regulatory pathway (Supplementary Fig. 1) that involves bidirectional cell signalling mediated by miRNA165/6 (miR165/6) and the transcription factors SHORT ROOT (SHR) and SCARECROW (SCR) controlling xylem patterning.

Endodermal SHR controls xylem patterning

SHR is produced in the stele and moves into the endodermis to activate *SCR*11¯15. In mutants of *SHR* or *SCR*, the asymmetric cell division that forms endodermis and cortex fails to occur and the quiescent centre is not maintained, resulting in short roots with only one ground tissue layer12,16,17. Despite the endodermal-specific expression of *SCR* genome-wide mRNA profiling of wild-type, *shr* and *scr* roots14,15 (Methods) indicated that nearly half of the genes co-regulated by *SHR* and *SCR* were expressed at the highest level in the stele (Supplementary Fig. 2). Furthermore, in both *scr* and *shr* mutants, metaxylem differentiates ectopically in the place of proto-xylem (Fig. 1e, f, g), indicating that SHR and SCR affect stele development in a non-cell autonomous manner.

Because SHR is normally present in both the stele and the endodermis, we determined where its activity is required for xylem patterning. We first expressed *SHR* strictly in the stele of *shr-2* by introducing a construct in which a non-mobile version of SHR18 containing a nuclear localization signal was driven by the stele-specific promoter of *CRE1* (ref. 19). Recovery of root meristem size (Student's *t*-test; $P < 0.001$, $\alpha = 0.05$) and root growth ($P < 0.001$, $\alpha = 0.05$) showed that this version of SHR was functional. Although we observed more immature phloem sieve cells than in *shr-2* (Supplementary Fig. 3), protoxylem formation was not rescued (Fig. 1b). We then expressed *SHR* strictly in the ground tissue by introducing *UAS::SHR:YFP* into *shr-2* harbouring *J0571*, an enhancer trap line that drives expression specifically in the ground tissue (www.plantsci.cam.ac.uk/Haseloff/; Fig. 1c and Supplementary Fig. 4). In addition to multiple ground tissue cell divisions, protoxylem formation was observed in 73% (24 of 33) of the lines (Fig. 1c), compared with 14% in *shr-2 J0571* alone. When *SCR* was expressed in the ground tissue in the absence of SHR, neither protoxylem nor endodermis was rescued

(Fig. 1d). Therefore, xylem patterning requires both SHR and SCR to be present in the endodermis.

Xylem patterning requires *PHB* restriction

In a screen for altered vascular development (Supplementary Fig. 5) we identified a mutant with a short root and frequent differentiation of metaxylem in place of protoxylem (Fig. 1h). This mutant had a point mutation in the miR165/6 target site in the class III homeo-domain leucine zipper (HD-ZIP III) gene *PHABULOSA* (*PHB*). Consistent with the phenotype of this new allele, *phb-7d*, the strong gain-of-function allele *phb-1d* (ref. 20) invariably formed ectopic metaxylem (Supplementary Fig. 5e).

Comparison of vascular development using cell and tissue markers reinforced the striking similarity of the *phb-7d* and *shr-2* phenotypes (Supplementary Fig. 6 and Supplementary Table 1). To determine if the *phb-7d* phenotype was caused by reduced SHR activity, we expressed the green fluorescent protein fusion *SHR::SHR:GFP*13 in *phb-7d* (Supplementary Fig. 7) but found no deviation from wild-type expression, indicating that this was unlikely.

As expected if the *phb-7d* mutation renders the *PHB* transcript resistant to miRNA-mediated degradation, its mRNA levels were elevated in the mutant (Supplementary Fig. 5d). RNA *in situ* hybridization in wild type showed that *PHB* mRNA localized primarily to the metaxylem precursors and neighbouring procambial cells, and at a residual level in protoxylem precursors (Fig. 2a). In *phb-7d* the *PHB* mRNA domain expanded throughout as well as outside the stele (Fig. 2b), indicating that miR165/6 normally acts to exclude *PHB* mRNA from the stele periphery and ground tissue.

The importance of miRNAs in xylem cell specification was supported further by the ectopic metaxylem phenotype of the mutant of HYL1, which specifically binds the miRNA during miRNA-mediated mRNA degradation21‚22 (Supplementary Fig. 8). We did not detect ectopic metaxylem in mutants of several well-characterized genes in the si- and tasiRNA-mediated RNA degradation pathways, indicating that xylem patterning is primarily mediated by miRNAs.

SHR post-transcriptionally represses PHB

Genome-wide expression profiling of *shr*, *scr* and wild-type roots indicated that *PHB* and the other four *HD-ZIP III* genes targeted by miR165/6 (refs 23–25) are upregulated in the *shr* and *scr* mutant backgrounds (Supplementary Fig. 9). To characterize further the relationship between SHR and the HD-ZIP III transcription factors we crossed *shr-2* with loss-of-function mutants of three HD-ZIP III transcription factors, *PHB*, *PHAVOLUTA* (*PHV*) and *REVOLUTA* (*REV*), which are closely related and functionally redundant in leaf development23. The *phb-6 phv-5 rev-9* mutant did not show any major deviation in xylem patterning26 from wild-type roots (Supplementary Figs 10 and 19). However, in the *phb-6 phv-5 rev-9 shr-2* quadruple mutant, the xylem patterning defect of *shr* was completely rescued (Supplementary Fig. 10). This provides strong evidence that ectopic metaxylem formation in *shr* is the result of upregulation of at least one of these HD-ZIP III transcription factors. This quadruple mutant also largely rescued the number of vascular cell files and root length (Supplementary Fig. 10). Analysis of the segregating double mutants showed that *phb shr* fully recovered protoxylem (in about 80%) and root growth, whereas *phv shr*, *rev shr* and *phv rev shr* did not (Fig. 1i and Supplementary Figs 10 and 11). Loss-of-function mutations in the two other *HD-ZIP III* genes, *ATHB8* and *CORONA/ATHB15* (*CNA*) could not restore the root growth of *shr-2*, but in both double mutants, *athb8-11 shr-2* and *cna-2 shr-2*, stretches of protoxylem were infrequently observed (Supplementary Fig. 11). Combining mutation in *phb* with *scr* also fully recovered protoxylem (Supplementary Fig.

11). Hence, these genetic analyses indicate that *SHR/SCR* repression of *PHB* is the primary pathway for xylem patterning.

We asked whether PHB was repressed by SHR at the transcriptional or post-transcriptional level. For this we analysed transcriptional (*PHB::GFP*) and translational GFP fusions (*PHB::PHB:GFP*) driven by the *PHB* promoter27. Patterns of *PHB::GFP* indicated that *PHB* is transcribed throughout the stele and endodermis (ground tissue in *shr*) in both wild-type and *shr* root meristems (Fig. 2f), whereas *PHB::PHB:GFP* was restricted to the central vascular cylinder in wild type (Fig. 2h). When the *phb-7d* mutation was introduced into the cDNA of the translational fusion, the GFP domain became similar to the *PHB* transcriptional domain in wild type (Fig. 2i). In *shr*, *PHB::PHB:GFP* and *PHB* mRNA domains expanded throughout the stele, similar to the pattern of *PHB::GFP* (Fig. 2g, h). These data indicate that SHR restricts PHB at the post-transcriptional level.

These results further implied that the meristematic zone is where PHB determines the root xylem cell types. Supporting this, we found that a miRNA-resistant version of *PHB* (with a silent mutation) expressed in the meristematic region under the stele-specific *CRE1* promoter was sufficient for ectopic metaxylem to form both in wild type and in the *phb shr* double mutant (Supplementary Fig. 12).

In summary, our data indicate that miR165/6 post-transcriptionally restricts *PHB* within the root meristem to the stele centre for proper xylem patterning and that SHR regulates this process by promoting miR165/6 activity in the stele periphery and endodermis.

SHR activates miR165/6 in the endodermis

We compared levels of miR165/6 in root tips of *shr*, *scr* and wild type. In *shr*, miR165/6 levels were reduced eightfold, and in *scr* threefold compared to wild type (Supplementary Fig. 13; Methods). Comparison of gene expression profiles of components related to small RNA pathways in whole roots14,15 showed no statistically significant expression changes in these mutant backgrounds (Supplementary Table 2), indicating that *SHR* and *SCR* primarily control miR165/6 activity by regulating *MIR165/6* expression.

To determine which of the *MIR165/6* genes are controlled by *SHR* and *SCR*, expression patterns of transgenic promoter::GFP (endoplasmic reticulum-localized) lines with the complete intergenic region of eight of the *MIR165/6* genes (except *165b*) were analysed in wild type, *shr-2* and *scr-1* (Fig. 3a, b and Supplementary Fig. 14). Only *MIR165a* and *166b* promoters drove detectable GFP in distinct patterns in wild-type roots. We note that another study28 suggests that *MIR166a* is also expressed at low levels in roots. *pMIR165a::GFP* showed endodermis-specific expression throughout the root (Fig. 3a), whereas *pMIR166b::GFP* was expressed strongly in the endodermis and quiescent centre and weakly in cortex and epidermis of the meristems of embryonic, primary and lateral roots (Fig. 3b and Supplementary Fig. 14). In *shr* roots, GFP was not detected from *pMIR165a::GFP* in any tissue, and only low-level activity was observed in the ground tissue and epidermis from *pMIR166b::GFP* (Fig. 3b and Supplementary Fig. 14). The constructs behaved similarly in *scr*, showing marked reduction in expression, with the exception that *pMIR165a::GFP* was detected in the ground tissue from the late maturation zone (Fig. 3a, b and Supplementary Fig. 14). As in wild type, GFP driven by any of the other six promoters could not be detected in *shr* roots. Consistent with the GFP data, real time PCR with reverse transcription analysis (RT–PCR) indicated significant reduction of pri-*MIR165a* and pri-*MIR166b* in both *shr* and *scr* roots (Supplementary Fig. 13).

To determine whether SHR is a direct regulator of *MIR165/6* we performed chromatin immunoprecipitation (ChIP) followed by real-time quantitative PCR (Methods). We

reproducibly found enrichment of fragments approximately 1 kb upstream of the transcription start site of *MIR165a*, 4.5 kb upstream of *MIR166b* (Fig. 3c), and 2.5 kb upstream of *MIR166a* (data not shown). Taken together, our data indicate that SHR activates transcription of *MIR165a* and *166b* in the endodermis directly.

miR165/6 acts non-cell-autonomously

We reported previously that the *HD-ZIP III* transcriptional domains are largely restricted to the vascular cylinder27. *PHB* is the only one whose transcriptional domain partially overlaps with the endodermal activity domain of *SHR* and *SCR*. Hence, for miR165/6 produced in the endodermis to encounter *HD-ZIP III* mRNA in the stele, there must be a mobile signal.

To understand the nature of this non-cell autonomous regulation, we first compared the spatial distribution of miR165/6 activity in wild-type and *shr-2* roots using a 'miRNA-sensor'29 (Fig. 4a; Methods). In this system, high miR165/6 activity is reflected by low GFP expression. Without the miRNA recognition site the GFP levels were uniform in the stele in both wild type and *shr*. In wild-type roots the sensor GFP with the miRNA recognition site was significantly lower in the ground tissue and stele periphery than in other cell types, consistent with the observed reduction in the *PHB* mRNA and protein domains in wild type. In *shr-2*, the sensor GFP expression level was uniform throughout the root.

Second, we determined the spatial distribution of mature miR165/6 in the root meristem of wild type and *shr* using *in situ* hybridization with locked nucleic acid (LNA) probes (Fig. 4b and Supplementary Fig. 15; Methods). In wild-type meristems, mature miR165/6 was detected at a low level in the quiescent centre and surrounding cells, but became progressively higher and ubiquitous throughout the root radius 30–40 μm distal from the quiescent centre. In cells close to the quiescent centre, mature miR165/6 levels were considerably higher in the cortical and epidermal cell layers than in the endodermis and stele cells. Hence, the pattern seemed complementary to the domain of *PHB* transcription. A complementary pattern of a mature miRNA and its target is consistent with previous observations30, but rather contradictory to our results showing the highest promoter activity of *MIR165a* and *MIR166b* in the endodermis. We proposed that the hybridization signal may reflect mainly the distribution of free miR165/6. Consistent with this, we detected less of a differential distribution of miR165/6 in the *phb-13* mutant and in several loss-of-function *HD-ZIP III* mutants where target mRNA is very low or absent. In these backgrounds the miR165/6 signal became high and ubiquitous throughout the root radius, even in tissues close to the quiescent centre (Fig. 4b and Supplementary Fig. 15). In *shr-2*, the miR165/6 pattern was similar to wild type, but at a markedly lower level, probably reflecting the residual expression of *MIR166b* (Fig. 4b). Hence, the sensor and *in situ* hybridization results indicate that the mature miRNA165/6 moves radially both outward and inward from the endodermis.

Third, we drove *MIR165a* expression by a ground-tissue-specific promoter (*shr-2 J0571; UAS::MIR165a*) in *shr* and observed the resulting xylem pattern (Fig. 4c and Supplementary Fig. 4). Five independent segregating T2 lines showed a clear recovery of protoxylem (Fig. 4c) at frequencies ranging from 33% to 88%, accompanied by suppression of mRNA levels of all the *HD-ZIP III*s (Fig. 4d) and restriction of *PHB* and *CNA* mRNA domains within the stele (Supplementary Fig. 16). Co-segregation of protoxylem formation with the activator was verified by backcrossing. Similarly, both *J0571* ≫ *MIR165a* (Fig. 4c) in *scr-4* and *MIR165a* expressed under another ground-tissue-specific promoter, *pSCR*, in the *scr-6* allele, rescued protoxylem formation (Supplementary Fig. 17).

Further support for this hypothesis is that protoxylem recovery observed when *SHR* was specifically expressed in the ground tissue of *shr* (Fig. 1c) was accompanied by an increase

in *MIR165a* and *166b* levels, and a decrease in mRNA levels of all five *HD-ZIP III* genes (Supplementary Fig. 18a), whereas SHR exclusively localized to the stele of the *shr* mutant did not affect either miR165/6 or *HD-ZIP III* mRNA levels (Fig. 1d and Supplementary Fig. 18b). Taken together, our results strongly support that miR165/6 in the endodermis mediates the non-cell-autonomous action of *SHR* and *SCR* in xylem patterning, by moving into the stele to restrict the *HD-ZIP III* mRNA domains.

HD-ZIP III levels determine xylem type

Our results indicated that PHB was the primary determinant, but other HD-ZIP IIIs may have a role in metaxylem specification as well. To investigate further the role of all five *HD-ZIP III* genes in root vascular patterning, we analysed their expression and assessed their loss-of-function phenotypes. Similar to *PHB*, *CNA* and *ATHB8* were expressed in xylem precursor cells (Fig. 2c, d): *CNA* in the metaxylem domain and neighbouring procambial cells and *ATHB8* specifically in the xylem axis including the protoxylem precursors. *REV* was broadly expressed in the vascular tissue just above the quiescent centre (Fig. 2e), but disappeared from the metaxylem domain farther away from the quiescent centre. *PHV* mRNA was not detected. In summary, the *HD-ZIP III* mRNA levels in the root meristem appear highest in the centre of the xylem axis and become lower towards the stele periphery.

In contrast with ectopic *PHB* expression, which causes central metaxylem fate in the stele periphery, the loss of combinations of *HD-ZIP III* genes resulted in protoxylem differentiating in the central metaxylem positions or even abolished xylem differentiation entirely (Fig. 5 and Supplementary Fig. 19). This is consistent with previous studies showing that HD-ZIP III transcription factors may direct xylem development23,25,31–33. All single and most double mutants displayed normal xylem patterning. However, the *athb8-11 phb-13* and various triple mutants had ectopic protoxylem partly replacing metaxylem. When four of the five genes were mutated no metaxylem was observed in any of the mutant combinations examined. Consistent with changes in xylem cell fates, low or no expression of the metaxylem marker gene *ACL5* (ref. 34) and ectopic expression in the centre of the xylem axis of the protoxylem marker *AHP6* (ref. 35) were observed in *athb8-11 cna-2 phb-13 phv-11* (Supplementary Fig. 20). This mutant also generated more vascular cells and, in contrast to the invariably diarch vascular arrangement in wild type, often formed a tri- or tetrarch arrangement, indicating that the *HD-ZIP III* genes redundantly restrict vascular cell proliferation (Supplementary Fig. 19). Surprisingly, loss of all five HD-ZIP III transcription factors failed to form any xylem (Fig. 5b). Partial failure in xylem differentiation was also detected in certain quadruple mutants (Supplementary Fig. 19). These results show that expression levels of HD-ZIP III transcription factors determine not only xylem cell types, but also *de novo* formation of xylem.

Finally, we increased the level of miR165 throughout the stele in wild type and *shr-2*. In both backgrounds an increased number of stele cells was observed (not shown) and all xylem precursors acquired peripheral fate differentiating exclusively as protoxylem (Fig. 5c, d), similar to the phenotypes of several multiple loss-of-function *HD-ZIP III* mutants. Thus, xylem patterning requires suppression of *HD-ZIP III* mRNA in the stele periphery through the activity of miR165/6.

Discussion

Our study highlights a novel regulatory pathway that integrates transcriptional and post-transcriptional regulation and bidirectional cell-to-cell communication to drive tissue patterning in the *Arabidopsis* root (Supplementary Fig. 1). Formation of vascular tissue with a surrounding endodermal layer was a key milestone in the evolution of land plants17,18.

Our study shows that its underlying regulation involves evolutionarily conserved SHR/SCR and HD-ZIP III transcription factors, and miR165/6 (refs 36, 37), implying that this regulatory mechanism might underlie the evolutionary adaptation to terrestrial growth.

The mobility of miR165/6 in the shoot apical meristem has been suggested previously[2–6]. Our study indicates that miR165/6 is mobile in the root and its mobility over a short distance is critical for dosage-dependent regulation of HD-ZIP III transcription factors in xylem patterning. A recent modelling study indicates that a mobile small RNA can sharpen the boundary of the activity domain of its target[38]. Our study shows that this may be the role for the endodermally produced miR165/6 as it moves into the vascular cylinder to encounter its target mRNA, thereby communicating radial positional information between cells of the root meristem.

METHODS SUMMARY

For anatomical and histological analyses, primary roots of vertically grown 4 to 5-day-old seedlings were used. Plastic sectioning, basic fuchsin staining and confocal imaging were performed as described[19].

For quantification of mRNA and miRNA, root tips from 6- to 7-day-old seedlings were collected and total RNA including small RNAs was extracted with an miRNeasy Mini kit (Qiagen). To measure the expression level of pri-miRNA and other mRNAs, cDNA was synthesized using SuperScript III first strand synthesis system for RT–PCR (Invitrogen). For mature miRNA, a polyadenylation reaction was performed before the reverse transcription following the method of ref. 39. Differences in gene expression were measured by real time PCR using an ABI 7900HT (Applied Biosystems).

Sectioning, preparation of riboprobes and *in situ* hybridization were performed as described[19]. LNA probes with complementary sequences to miR165 and miR166 were synthesized, 5′ digoxigenin-labelled (Exiqon), and then hybridized at 50 °C.

Most transgenic constructs were generated using the modified multisite gateway system[27] and all were introduced into plants using the floral dip method[40].

To identify *in vivo* binding activities of SHR to the promoters of *MIR165/6*, plants expressing *SHR::SHR:GFP* in *shr-2* were used. Roots were collected 6 days after germination and processed for ChIP[14]. SHR binding affinity was compared between the ChIP DNA treated with and without GFP antibody by measuring the differential enrichment of DNA fragments using real-time PCR.

Supplementary Material

Refer to Web version on PubMed Central for supplementary material.

Acknowledgments

We thank K. Kainulainen, M. Herpola, G.-B. Berglund and J. Jung for technical assistance; M. Prigge, S. Clark, C. Bellini, N. Sauer, J. Colinas, T. Vernoux, K. Gallagher, A. P. Mahonen, A. Bishopp, M. Bonke, N. Fedoroff, J. C. Fletcher, B. J. Reinhart, I. Pekker, ABRC and NASC for materials, and E. Richards and M. Harrison for comments on the manuscript; M. Tsiantis for sharing results before publication. This work was supported by the Boyce Thompson Institute and NSF IOS0818071 to J.-Y.L., Cornell Presidential Life Science Fellowship to J.Z., grants from the NIH (RO1-GM043778) and from the NSF *ARABIDOPSIS* 2010 programme to P.N.B., a fellowship from the MICINN, Spanish Government to M.A.M.-R., grants by the Academy of Finland, Tekes and ESF to Y.H., S.L. and A.V., European Molecular Biology Organisation (EMBO, ALTF 450-2007) to J.D., Estonian funding agencies (ETF7361 and SF0180071s07) to O.L., Nilsson-Ehle Foundation to C.J.R, and FORMAS and Carl Trygger's

Foundation for Scientific Research to A.C. Imaging at Boyce Thompson Institute was supported by NSF (NSF DBI-0618969) and Triad Foundation.

References

1. Du TG, Schmid M, Jansen RP. Why cells move messages: The biological functions of mRNA localization. Semin Cell Dev Biol. 2007; 18:171–177. [PubMed: 17398125]
2. Tretter EM, Alvarez JP, Eshed Y, Bowman JL. Activity range of *Arabidopsis* small RNAs derived from different biogenesis pathways. Plant Physiol. 2008; 147:58–62. [PubMed: 18443104]
3. Dunoyer P, Himber C, Ruiz-Ferrer V, Alioua A, Voinnet O. Intra- and intercellular RNA interference in *Arabidopsis thaliana* requires components of the microRNA and heterochromatic silencing pathways. Nature Genet. 2007; 39:848–856. [PubMed: 17558406]
4. Chitwood DH, et al. Pattern formation via small RNA mobility. Genes Dev. 2009; 23:549–554. [PubMed: 19270155]
5. Nogueira FTS, et al. Regulation of small RNA accumulation in the maize shoot apex. PLoS Genet. 2009; 5:e1000320. [PubMed: 19119413]
6. Juarez MT, Kui JS, Thomas J, Heller BA, Timmermans MCP. microRNA-mediated repression of *rolled leaf1* specifies maize leaf polarity. Nature. 2004; 428:84–88. [PubMed: 14999285]
7. Lin SI, et al. Regulatory network of microRNA399 and *PHO2* by systemic signaling. Plant Physiol. 2008; 147:732–746. [PubMed: 18390805]
8. Esau, K. Anatomy of Seed Plants. 2. Wiley; 1977.
9. Pryer, KM.; Schneider, H.; Magallón, S. Assembling the Tree of Life. Cracraft, J.; Donoghue, MJ., editors. Vol. Ch 10. Oxford Univ. Press; 2004. p. 138-153.
10. Kevin Boyce, C.; Holbrook, NM.; Maciej, AZ. Vascular Transport in Plants. Academic Press; 2005. p. 479-499.
11. Gallagher KL, Paquette AJ, Nakajima K, Benfey PN. Mechanisms regulating SHORT-ROOT intercellular movement. Curr Biol. 2004; 14:1847–1851. [PubMed: 15498493]
12. Helariutta Y, et al. The *SHORT-ROOT* gene controls radial patterning of the *Arabidopsis* root through radial signaling. Cell. 2000; 101:555–567. [PubMed: 10850497]
13. Nakajima K, Sena G, Nawy T, Benfey PN. Intercellular movement of the putative transcription factor SHR in root patterning. Nature. 2001; 413:307–311. [PubMed: 11565032]
14. Cui H, et al. An evolutionarily conserved mechanism delimiting SHR movement defines a single layer of endodermis in plants. Science. 2007; 316:421–425. [PubMed: 17446396]
15. Levesque MP, et al. Whole-genome analysis of the SHORT-ROOT developmental pathway in *Arabidopsis*. PLoS Biol. 2006; 4:e143. [PubMed: 16640459]
16. Di Laurenzio L, et al. The *SCARECROW* gene regulates an asymmetric cell division that is essential for generating the radial organization of the *Arabidopsis* root. Cell. 1996; 86:423–433. [PubMed: 8756724]
17. Sabatini S, Heidstra R, Wildwater M, Scheres B. SCARECROW is involved in positioning the stem cell niche in the *Arabidopsis* root meristem. Genes Dev. 2003; 17:354–358. [PubMed: 12569126]
18. Gallagher KL, Benfey PN. Both the conserved GRAS domain and nuclear localization are required for SHORT-ROOT movement. Plant J. 2009; 57:785–797. [PubMed: 19000160]
19. Mähönen AP, et al. A novel two-component hybrid molecule regulates vascular morphogenesis of the *Arabidopsis* root. Genes Dev. 2000; 14:2938–2943. [PubMed: 11114883]
20. McConnell JR, et al. Role of *PHABULOSA* and *PHAVOLUTA* in determining radial patterning in shoots. Nature. 2001; 411:709–713. [PubMed: 11395776]
21. Han MH, Goud S, Song L, Fedoroff N. The *Arabidopsis* double-stranded RNA-binding protein HYL1 plays a role in microRNA-mediated gene regulation. Proc Natl Acad Sci USA. 2004; 101:1093–1098. [PubMed: 14722360]
22. Vazquez F, Gasciolli V, Cr P, Vaucheret H. The nuclear dsRNA binding protein HYL1 is required for microRNA accumulation and plant development, but not posttranscriptional transgene silencing. Curr Biol. 2004; 14:346–351. [PubMed: 14972688]

23. Emery JF, et al. Radial patterning of *Arabidopsis* shoots by class III HD-ZIP and KANADI genes. Curr Biol. 2003; 13:1768–1774. [PubMed: 14561401]
24. Mallory AC, et al. MicroRNA control of *PHABULOSA* in leaf development: importance of pairing to the microRNA 59region. EMBO J. 2004; 23:3356–3364. [PubMed: 15282547]
25. Zhou GK, Kubo M, Zhong R, Demura T, Ye ZH. Overexpression of miR165 affects apical meristem formation, organ polarity establishment and vascular development in *Arabidopsis*. Plant Cell Physiol. 2007; 48:391–404. [PubMed: 17237362]
26. Hawker NP, Bowman JL. Roles for class III HD-Zip and KANADI genes in *Arabidopsis* root development. Plant Physiol. 2004; 135:2261–2270. [PubMed: 15286295]
27. Lee JY, et al. Transcriptional and posttranscriptional regulation of transcription factor expression in *Arabidopsis* roots. Proc Natl Acad Sci USA. 2006; 103:6055–6060. [PubMed: 16581911]
28. Jung JH, Park CM. *MIR166*/*165* genes exhibit dynamic expression patterns in regulating shoot apical meristem and floral development in *Arabidopsis*. Planta. 2007; 225:1327–1338. [PubMed: 17109148]
29. Parizotto EA, Dunoyer P, Rahm N, Himber C, Voinnet O. *In vivo* investigation of the transcription, processing, endonucleolytic activity, and functional relevance of the spatial distribution of a plant miRNA. Genes Dev. 2004; 18:2237–2242. [PubMed: 15371337]
30. Stark A, Brennecke J, Bushati N, Russell RB, Cohen SM. Animal MicroRNAs confer robustness to gene expression and have a significant impact on 39UTR evolution. Cell. 2005; 123:1133–1146. [PubMed: 16337999]
31. Baima S, et al. The *Arabidopsis* ATHB-8 HD-zip protein acts as a differentiation-promoting transcription factor of the vascular meristems. Plant Physiol. 2001; 126:643–655. [PubMed: 11402194]
32. Ohashi-Ito K, Kubo M, Demura T, Fukuda H. Class III homeodomain leucine-zipper proteins regulate xylem cell differentiation. Plant Cell Physiol. 2005; 46:1646–1656. [PubMed: 16081527]
33. Prigge MJ, et al. Class III homeodomain-leucine zipper gene family members have overlapping, antagonistic, and distinct roles in *Arabidopsis* development. Plant Cell. 2005; 17:61–76. [PubMed: 15598805]
34. Muñiz L, et al. ACAULIS5 controls *Arabidopsis* xylem specification through the prevention of premature cell death. Development. 2008; 135:2573–2582. [PubMed: 18599510]
35. Mähönen AP, et al. Cytokinin signaling and its inhibitor AHP6 regulate cell fate during vascular development. Science. 2006; 311:94–98. [PubMed: 16400151]
36. Floyd SK, Bowman J. The ancestral developmental tool kit of land plants. Int J Plant Sci. 2007; 168:1–35.
37. Floyd SK, Bowman JL. Gene regulation: ancient microRNA target sequences in plants. Nature. 2004; 428:485–486. [PubMed: 15057819]
38. Levine E, McHale P, Levine H. Small regulatory RNAs may sharpen spatial expression patterns. PLoS Comp Biol. 2007; 3:e233.
39. Shi R, Chiang VL. Facile means for quantifying microRNA expression by real-time PCR. Biotechniques. 2005; 39:519–525. [PubMed: 16235564]
40. Clough SJ, Bent AF. Floral dip: a simplified method for *Agrobacterium*-mediated transformation of *Arabidopsis thaliana*. Plant J. 1998; 16:735–743. [PubMed: 10069079]

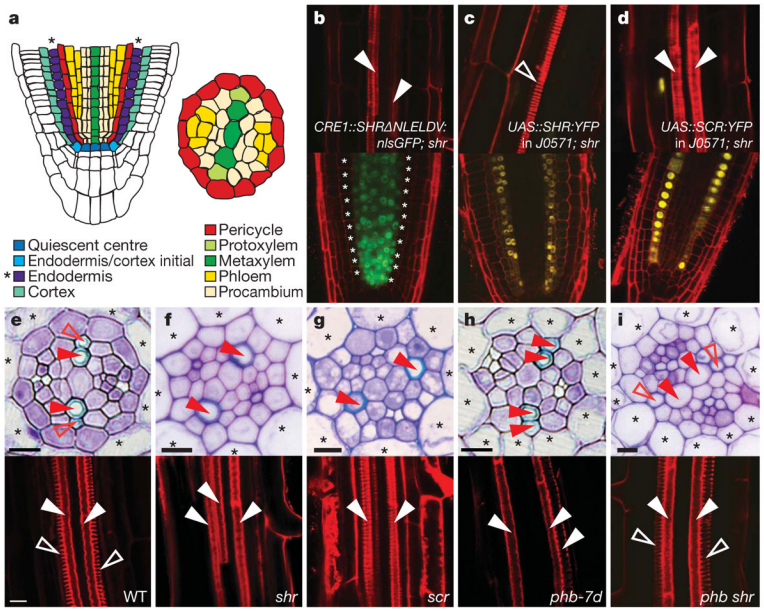

Figure 1. Endodermal SHR and SCR control xylem patterning via *PHB*

a, Schematic representation of the *Arabidopsis* root meristem and stele. Cells in the ground tissue layer adjacent to the stele are marked with asterisks. **b**, *CRE1::SHRΔNLELDV:nlsGFP* in *shr-2*. **c**, *UAS::SHR:YFP* in *shr-2* harbouring *J0571*. **d**, *UAS::SCR:YFP* in *shr-2*, *J0571*. **e**–**i**, Toluidine blue-stained cross-sections and confocal laser scanning micrographs of basic fuchsin-stained xylem of wild type (WT) (**e**), *shr-2* (**f**), *scr-4* (**g**), *phb-7d* (**h**), and *phb-6 shr-2* (**i**). Filled arrowhead indicates metaxylem, and unfilled indicates protoxylem. Scale bars, 10 μm.

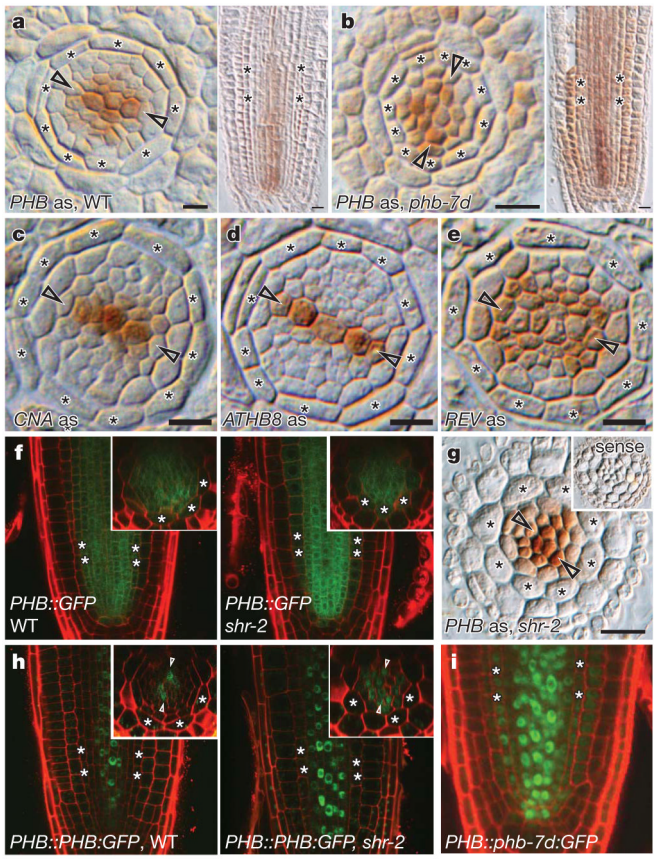

Figure 2. SHR post-transcriptionally represses *PHB*

a, **b**, *In situ* hybridization with a *PHB* mRNA specific probe on cross- and longitudinal sections of WT (**a**) and *phb-7d* (**b**) roots. **c**–**e**, *In situ* hybridization with *CNA* (**c**), *ATHB8* (**d**) and *REV* (**e**) specific probes on cross-sections of WT roots. **f**, Confocal laser scanning micrographs of transcriptional fusion of *PHB* to GFP in WT and *shr-2*. **g**, *PHB* mRNA *in situ* hybridization to cross-section of *shr-2*. Inset is a section of *shr-2* hybridized with a *PHB* sense probe. **h**, Expression of translational fusion of *PHB* to *GFP* in WT and *shr-2*. **i**, Expression of translational fusion of *PHB* with the *phb-7d* mutation to *GFP*. Asterisks, endodermis position; arrowheads, protoxylem position; scale bars, 10 μm.

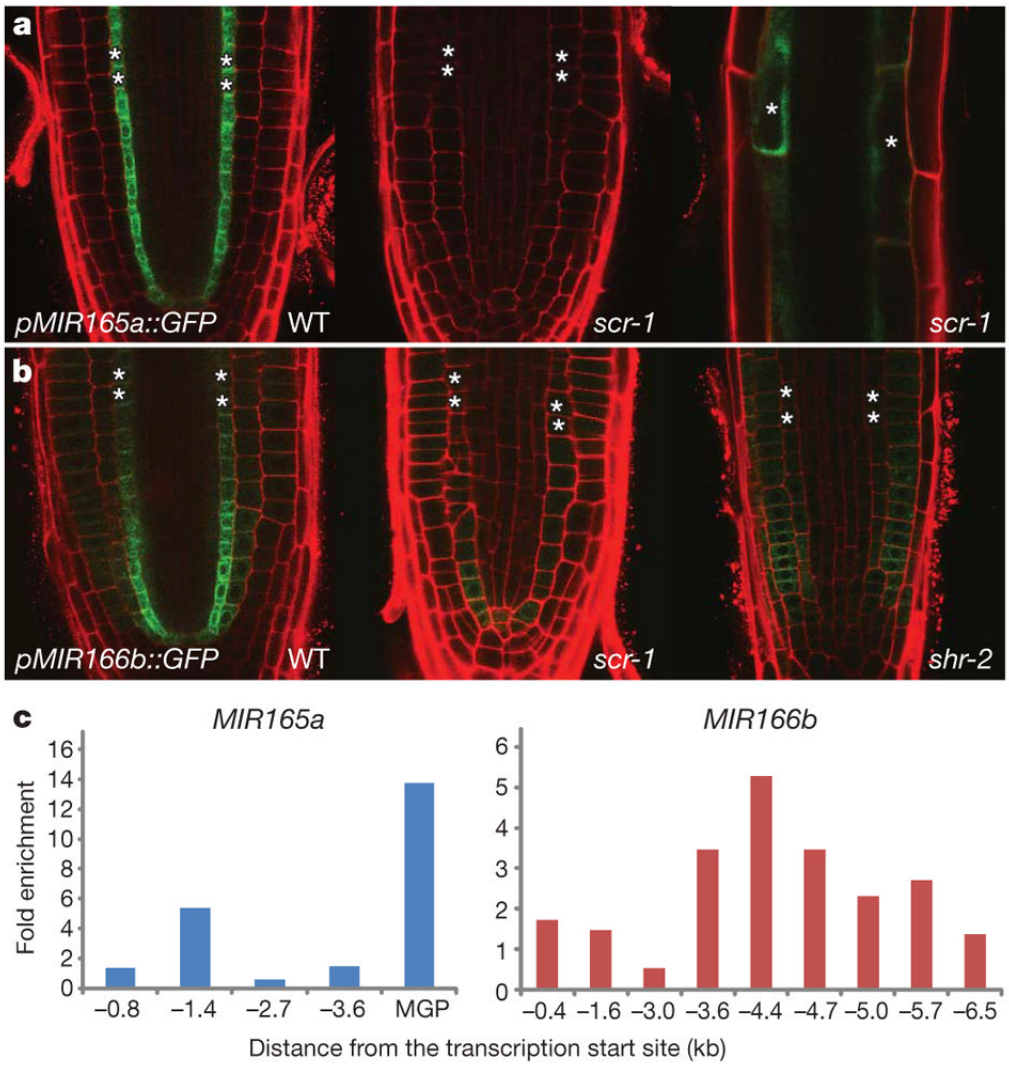

Figure 3. miR165/6 activated by SHR inthe endodermis is active in the stele

a, Expression of *pMIR165a::GFP* in WT and *scr-1* meristems and in maturation zone. **b**, Expression of *pMIR166b::GFP* in WT, *scr-1* and *shr-2* meristems. **c**, Real-time PCR of ChIP on the upstream regulatory regions of *MIR165a* and *MIR166b* using anti-GFP antibodies and a transgenic plant expressing *pSHR::SHR:GFP*. The binding to the *MAGPIE* (*MGP*) promoter confirmed previously21 was used as positive control. Asterisks, endodermis position.

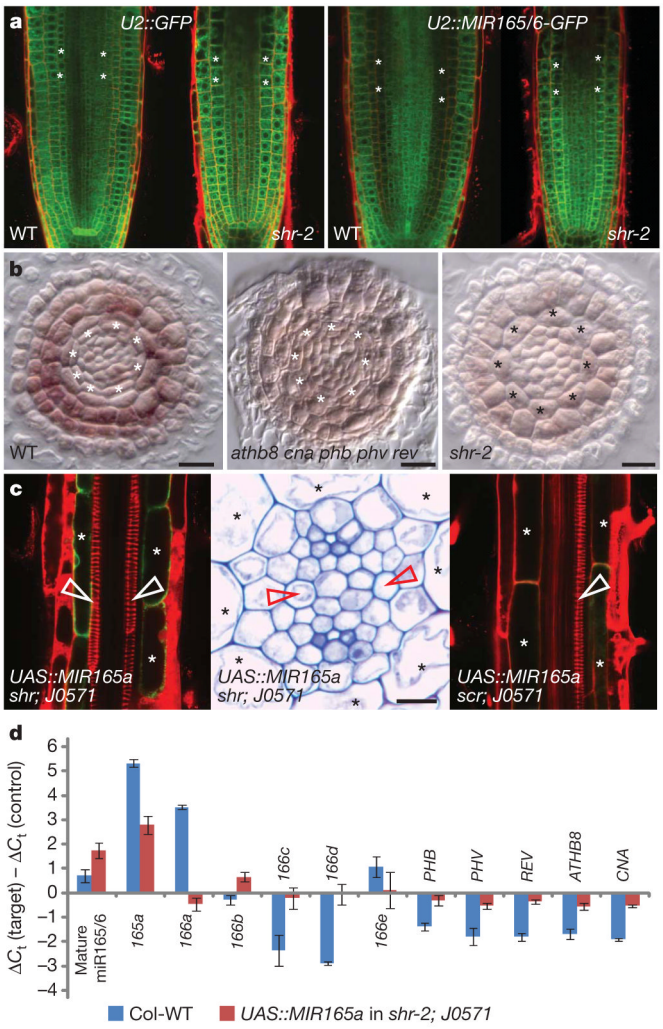

Figure 4. Non-cell-autonomous action of *MIR165a.*

a, miR165/6 GFP sensor under the U2 promoter in WT and *shr-2*. **b**, miR166-specific LNA probe hybridization to sections proximal to the quiescent centre of WT, *athb8-11 cna-2 phb-13 phv-11 rev-6* and *shr-2*. **c**, Protoxylem forms in *shr* and *scr* backgrounds when *UAS::MIR165a* is introduced into *shr-2* and *scr-4* harbouring *J0571*. **d**, Real-time RT–PCR of pri-*MIR165/6* and *HD-ZIP III* in WT and a line with *UAS::MIR165a* in *shr-2*, *J0571*. *n* 54. Error bars indicate ±s.d. Asterisks, endodermis/ground tissue position; arrowheads, protoxylem position; scale bars, 10 μm.

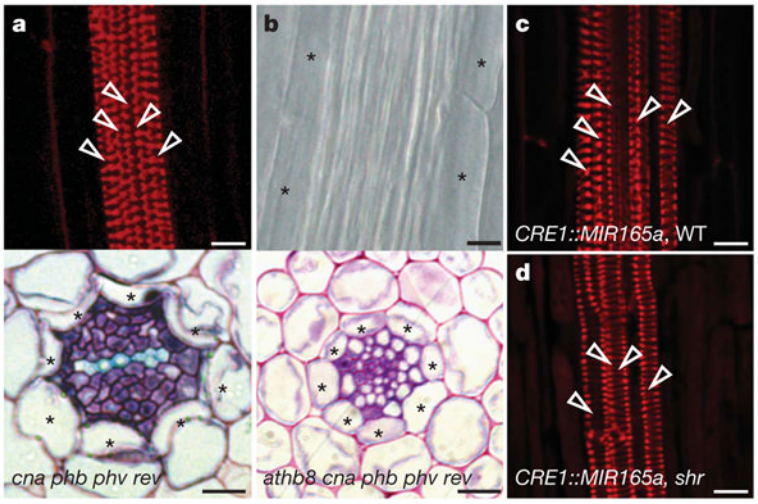

Figure 5. HD-ZIP III levels determine xylem type

a, Basic fuchsin-stained xylem and cross-section of *cna-2 phb-13 phv-11 rev-6*. **b**, Cleared root and cross-section of *athb8-11 cna-2 phb-13 phv-11 rev-6*. **c**, **d**, Stained xylem of roots in which *MIR165a* is expressed from the *CRE1* promoter in WT and *shr-2*. Asterisks, endodermis position; arrowheads, protoxylem position; scale bars, 10 μm.